Archaeological prospection in Chapingo, Texcoco Region, Mexico

Alejandro Rosado-Fuentes*
Alejandra Arciniega-Ceballos**

Recibido en septiembre de 2016; aceptado en diciembre de 2016

Resumen

Se aplicaron técnicas geofísicas no destructivas en el sitio arqueológico de Chapingo ubicado en la Región de Texcoco, México. El estudio combina la aplicación de Tomografía de Refracción Sísmica y Magnetometría con el fin de identificar y diferenciar estructuras de origen geológico y arqueológico en los primeros 10 m de profundidad del subsuelo. Los resultados y las características de las anomalías sísmicas y magnéticas sugieren la presencia de diversas estructuras que pueden ser un pozo de agua, canales de tránsito o riego, diques, y montículos o tlateles. Los resultados indican también indican la presencia de un lecho de un río con orientación SE-NW. Basándonos en las historias geológica y humana de la región, suponemos que el río data del periodo prehistórico, y que las otras estructuras son de origen prehispánico y/o colonial. Nuestros hallazgos muestran que la combinación de técnicas geofísicas es una herramienta precisa, detallada y de alta resolución apropiada para resolver problemas arqueológicos y de ingeniería civil.

Palabras clave: tomografía de refracción sísmica, magnetometría, prospección arqueológica, Texcoco, tlatel.

Abstract

A shallow non-destructive geophysical survey was conducted in the archaeological site of Chapingo in the Texcoco Region, Mexico. The survey combines the application of Seismic Refraction Tomography and Magnetometry in order to identify and differentiate geological and archaeological features in the first 10 m of the subsoil. The results and the characteristics of the seismic and the magnetic anomalies depicte features suggesting the presence of structures like a water-well, transit or irrigation channels, dams and mounds or tlatels. A SE-NW oriented riverbed was also identified. Based on the geologic and human histories of the region, we suppose the riverbed dates from the Pre-Historic period, and that the other structural features have a Pre-Hispanic and/or Colonial origin. Our findings exemplify that the combination of geophysical tech-niques is a precise,

* *Posgrado en Ciencias de la Tierra, Instituto de Geofísica, Universidad Nacional Autónoma de México. Circuito Exterior s/n. Zona de Institutos, Cd. Universitaria, Ciudad de México 04510, Mexico. arosadof@ciencias.unam.mx*
** *Departamento de Vulcanología, Instituto de Geofísica, Universidad Nacional Autónoma de México. Circuito Exterior s/n. Zona de Institutos, Cd. Universitaria, Ciudad de México 04510, Mexico. maac@geofisica.unam.mx*

detailed and high-resolution tool appropriate to solve ar-chaeological and civil engineer problems.

Key words: seismic refraction tomography, magnetometry, archaeological prospection, Texcoco, tlatel.

Introduction

The application of geophysical techniques is relevant for identifying and locating archaeological and structural remains for two main reasons: 1) the need to preserve the cultural heritage of a nation and 2) the effects on the stability of modern structures. Specially, in lacustrine areas like the Basin of Mexico, in which the Texcoco Region is located, buried structures modify the behavior of the subsoil. For instance, Padilla y Sánchez (1989) showed a link between more than 2000 collapsed and damaged buildings in Mexico City during the earth-quakes of September 1985 and the Pre-Hispanic and Colonial underneath structures.

In the region of Texcoco some archaeological remains have been found, dating 9730 $\pm$ 65 yr BP (Arciniega et al. 2009, González et al. 2001, Morett-Alatorre and Cabrales 2003, Parson 1971, Parsons and Morett-Alatorre 2004, Pompa y Padilla 2006, Siebe et al. 1999). Although this region is one of the most populated areas in Central Mexico since ancient times, the information of certain sites is limited and scarce. Recently, some Pre-Hispanic remains were discovered during a water pipe installation in a terrain of the Chapingo Autonomous University (UACh). The findings include drainage canals, postholes, human burials and the presence of mud bricks and ceramics dating to approximate 300 to 1100 AD. In addition, a Teotihuacan horizon (1.8 *m* thick) composed of sediments deposited over 900 years and a wavy surface interpreted as a tilled terrain, were identified (Morett-Alatorre – personal communication).

These findings motivated the application of non-destructive geophysical techniques to map geological and archaeological structures within the first 10 m of depth. In this work, we present the results of seismic and magnetic study conducted on a smallholding of the plantbreeding field San Martín, used by the UACh for experimental agricultural studies. First, we present a resume of the geological frame, followed by a brief history of human occupation in the region. Then we present the geophysical techniques applied and finally we describe fieldwork, data acquisition, analysis and interpretation of the results.

Geological frame

Mexico City´s Metropolitan Area (MCMA) is located within the endorheic Basin of Mexico on the Trans-Mexican Volcanic Belt (TMVB) between lati-tudes 20°04'02'' and 18°55'08'' N and longitudes 98°34'08'' and 99°39'06'' W, covering an area of 7661.06 km^2 (INEGI 2014a and 2014b). Most of MCMA lies on the lakebed of a practically extinct lacustrine system that had a total extension between 800

and 1000 km^2 (Rojas Rabiela 2004). This lacustrine system was essential for the development, evolution and sustainability of human settlements around it.

The Texcoco Region extends approximately 700 km^2, E of MCMA. It is confined to the W by Lake Texcoco´s shore, to N and E by the mountain ranges of Patlachique and Río Frio, respectively; and to the S by hills Chimalhuacan and Texolotl (Parsons 1971). Within the Texcoco Region, the city of Texcoco de Mora (Figure 1 top) is located 30 *km* NE of Mexico City (Arciniega et al. 2009) at 2250 m.a.s.l. (INEGI 2014b). Since 1923 the ChAU is established S of the city, in the former Hacienda Chapingo (Figure 1 middle).

Until the Cenozoic the region of the Basin of Mexico was covered by the sea, favoring the formation of the Texcoco Conglomerate. Uprisings of the continent from the Late Paleocene to the Early Eocene lead to the formation of the TMVB. The region was bordered counterclockwise by mountain ranges from the Sierra Nevada to the E to the Sierra de las Cruces to the W; this allowed the region to drain S into the Balsas River and later to the Pacific Ocean (Padilla y Sánchez 1989).

The Pleistocene-Holocene Chichinautzin mountain range closed the Basin to the S, and during the same period the Patlachique mountain range emerged (Mooser et al. 1974, Padilla y Sánchez 1989). The accumulation of water gave birth to a series of islets and to the lacustrine system composed by saltwater lakes Xaltocan, Zumpango and Texcoco, and freshwater lakes Xochimilco and Chalco. The weather characteristics of the region together with the precipitation and deposition rates of sediments, led to lakes with null circulation of water and high evaporation, such is the case of Lake Texcoco. This contrasts with the intermittent lakes in the western part of Lake Texcoco and crystal-clear lakes Chalco and Xochimilco (Padilla y Sánchez 1989).

Lake Texcoco was fed by rainfall, melting glaciers and several springs located in the vicinity. The environment and vegetation conditions were altered by strong contrast changes in salinity, depth and temperature due to a combination between weather and volcanic activity (Alcocer and Williams 1996, Lozano García and Ortega Guerrero 1998). Today, Lake Texcoco is at least 3.5 m higher than downtown Mexico City and it´s fed by a system of permanent and seasonal rivers (Alcocer and Williams 1996).

The shallow lakebed of Lake Texcoco consists of: a) a 3 m layer of clays followed by b) 25 m of interleaved layers of clay and silty sand, and then, c) a hard 3.5 m layer of silty sand, sand and silt and d) layers of consolidated silt and silty sands at approximately 42 m deep (Hortencia Flores et al. 2009). Paleontological sites in the region show lahars and mudflows interleaved with lacustrine sediments and ash layers, some being markers of Plinian eruptions (González et al. 2006, Morett Alatorre and Cabrales 2003, Siebe et al. 1999).

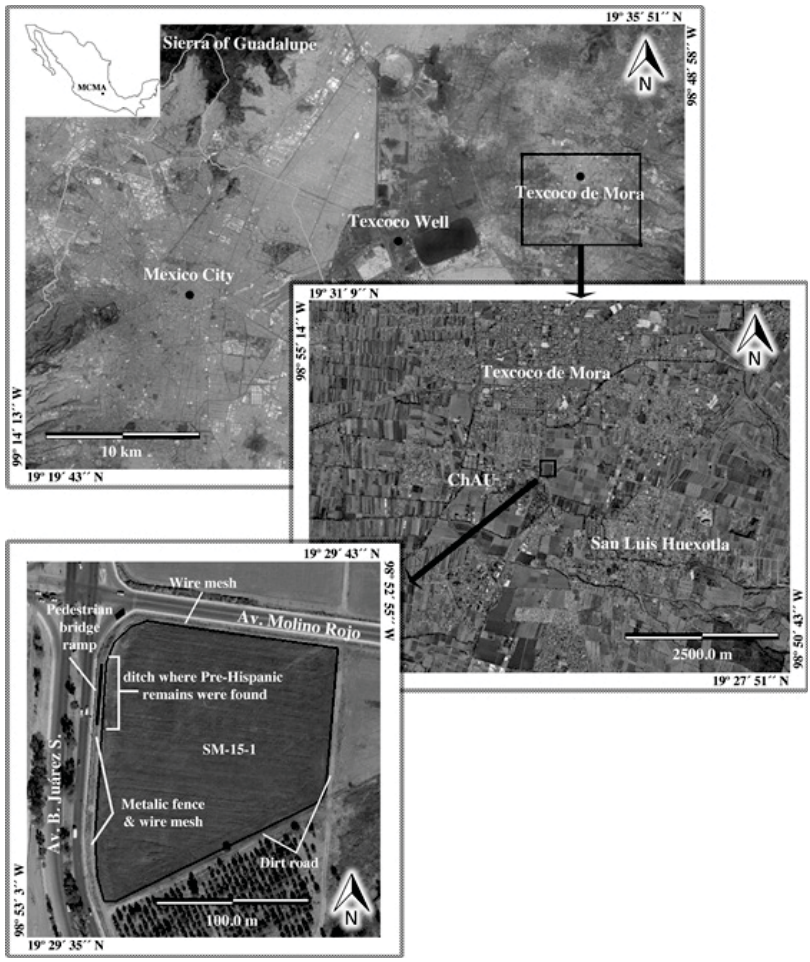

Figure 1. *Top: Google Earth satellite image of the NE region of MCMA. Middle: close-up of the Texcoco Region. Bottom: smallholding SM-15-1 of the ChAU.*

Human occupation history

The first nomadic groups arrived to the Basin of Mexico during the last glacia-tion (22000-14000 BP) (Polaco and Arroyo Cabrales 2001). This has been confirmed by findings of mega fauna remains association with human remains, man made artifacts or bones with signs of manufacturing processes (González et al. 2001 and 2006, Jiménez López et al. 2006, Morett Alatorre and Cabrales 2003, Pompa y Padilla 2006, Siebe et al. 1999). It is presumed that the extinction of mega fauna in the Late Pleistocene (González et al. 2006) incited the transition to sedentary

lifestyle and new forms of organization in the Early Preclassic (2500-1200 BC). It is also considered that this extinction might have led to the first human settlements in the Texcoco Region (Morett Alatorre and Cabrales 2003, García Moll 2007).

During the Middle and Late Preclassic (1200 BC-150 AD) population in the region grew partly due to the development of Teotihuacan and Cuicuilco. The construction of hydraulic systems helped to develop agriculture, which helped stop the dependence on seasonal rain (García Moll 2007, Pérez Campa 2007). According to Parsons (1971) 21 settlements – hunting sites, villages or towns – with a population estimate from 50 to more than 3500 habitants each, were located near our study site. Only seven of them had remains of a tlatel or mound. A tlatel is a Pre-Hispanic structure built through successive construction stages with stonewalls in-filled with rocks, silty sand and building debris. Depending on their dimensions they were used for domestic, residential or military purposes or as a ceremonial/civic center (Parsons 1971).

A migration towards establishments in the foothills of the Sierra Patlachique and Mount Portezuelo occurred during the Classic (150-650 AD) and Epiclassic (650-900 AD) (López Luján 2007, Nalda 2007). None of the 22 sites of these Eras had structural remains (Parsons 1971). Population continuously increased during the Postclassic and until the Spanish colonization (Matos Moctezuma 2007, Parsons 2007). Parsons (1971) identified 18 sites belonging to the Early and Middle Postclassic (900-1350 AD), but only three with mounds. In the Middle Postclassic the Acolhua civilization emerged and settled in the Texcoco Region; their capital city, Catlenihco, was founded in the XIII century. Later, it became known as Tetzcuco or Texcoco (Jarquín and Herrejón Peredo 2002). The area became very prominent and the Acolhuas dominated the region during the Late Postclassic (1350-1519 AD) and until the Spanish colonization. In this area, thirty one villages identified by Parsons (1971) present structural remains, most of them are associated with water channels. Out of the thirty-one sites, seven present mounds and four tlatels. Texcoco and Huexotla (Figure 1 bottom) were the principal urban areas of the region, their suburbs extended from the foothills of nearby mountains to Lake Texcoco. Parsons (1971) was able to identify eight ceremonial and three do-mestic tlatels in Texcoco; while in Huexotla he identified fourteen commercial and eighteen domestic tlatels plus other four whose purpose could not be de-termined.

Parsons and Morett Alatorre (2004) survey an area of circa 25 km^2 of Texcoco´s lakebed in 2003. During their expedition they located 1100 sites with archaeological remains in an area circa 25 km^2 dating back to the Postclassic and Epiclassic. These findings proved that the people of the Basin of Mexico used and exploited the resources of Lake Texcoco intensively for at least 1000 years and until the XX century. Here, we point out that the area of study is located between Texcoco and Huexotla, within the ChAU that is part of the former Hacienda Chapingo (see Figure 1 middle)

This Hacienda was founded in the late XVII century to supply goods to Mexico City (Jarquín and Herrejón Peredo, 2002). Within a century it grew to more than

13000 ha (Jarquín and Herrejón Peredo 2002, Rosas 2006). In 1884 president Manuel Gonzalez bought most of the hacienda and modernized it with electricity and a new railroad connecting Chapingo directly to Mexico City (Rosas 2006). In 1933 the National School of Agriculture moved into Chapingo and in the 70´s it was transformed into the ChAU, which up to date occupies the land of the former Hacienda (Jarquín and Herrejón Peredo 2002).

Geophysical Exploration Techniques

Archaeological prospection gives a glimpse of the structural remains on the subsoil; improving the excavation plan and reducing time and costs. It is very well known that geophysical exploration techniques are sensible to the changes of the physical properties of the subsoil (Telford et al. 1978). Magnetometry and Seismic Refraction Tomography (SRT) can be used to distinguish structures such as walls, mounds, ditches, pits, dikes and stoves (Arciniega et al. 2009, Fassbinder 2015). For their identification it is necessary to have information related to the characteristics of the materials in the area and the materials and techniques used for their construction (Cardarelli and Di Fillipo 2009). In one hand, magnetometry is one of the most used techniques in archaeological prospection (Fassbinder 2015) and on the other hand, SRT is not frequently used in archaeology because of its high cost and the necessary time for processing and to make a survey (Cardarelli and Di Filippo 2009, Telford et al.1978), however, SRT is the most efficient, precise and high-resolution technique. SRT can also be used to detect cavities within structures and different constructive stages (Arciniega et al. 2009, Cardarelli and Di Filippo 2009, Polymenakos et al. 2005). Below we briefly describe the main characteristics of each geophysical technique.

The magnetometry method is a passive technique that measures the geomagnetic field. The measured magnetic field is the sum of the principal field, the lithospheric field and the field generated by sources in the magnetosphere and ionosphere (Langel and Hinze 1998, Milsom 2003, Sharma 1978, Telford et al. 1978). Diurnal variations of Earth´s magnetic field are irregular and related to Sun Earth and Moon-Earth interactions, their effects cannot be predicted. These variations have to be removed from the data based on the available information obtained from monitoring observatories. The common way to do this is by using a diurnal base station situated on a well known area and far away from local sources of noise, such as modern constructions, vehicles, radio transmitters or power lines (Milsom 2003).

Structures with different magnetic properties than the subsoil enclosing them may change the local magnetic field producing an anomaly. These anomalies are caused by the contrast between the magnetization of rocks or soils containing oxides or ferromagnetic or ferrimagnetic minerals (David and Linford 2000, Langel and Hinze 1998, Milsom 2003). The anomaly or residual field is obtained by subtracting the calculated diurnal variation to the measured

magnetic field, this is also known as a diurnal correction (Langel and Hinze 1998). In an archaeological context for example, punctual anomalies can be associated with fires, filled holes and postholes, and linear anomalies can be associated walls or ditches (Fassbinder 2015).

On the other hand, SRT is an active geophysical technique that requires an artificial source to generate elastic waves. It is based on Snell´s Law and Fermat´s and Huygens´ Principles. The physical properties of the subsoil such as density, porosity or compaction determine the travel time of P-waves from the source to a geophone array located on the surface (Sharma 1978, Stein and Wysession 2003;, Telford et al. 1978). The distribution and geometry of the array depends on the objectives of the study and the depth of interest. Commonly the length of the array is more than three times the depth of interest (Aerona 2012, Obermann 2012).

Direct, reflected and refracted seismic waves travel from the source to a geophone following their corresponding path. After the crossover distance the first wave arriving at a geophone is the head wave or refracted wave, even though its path is longer than the travelled for the direct and reflected waves. SRT uses the first arrival of P-waves that were critically refracted by the interfaces found on its path. On each interface part of the energy will be set free at an angle equal to the critical angle (Stein and Wysession 2003). This technique assumes that the velocity increases with depth and it´s not sensible to low velocity layers or hidden layers between high velocity layers (Geometrics 2009, Milsom 2002, Stein and Wysession 2003).

The travel time curves are formed with the first arrivals readings and the source-receiver distance. These curves are inverted applying least squares and delay times to generate a two or three layer velocity model of the subsoil. This initial velocity model is meshed into a number of equivalent cells to calculate the travel paths, travel times and slowness of the P-waves (Forte and Pipan 2008, Geometrics 2009, Polymenakos et al. 2005, Stein and Wysession 2003). Then, a comparison between the observed and calculated travel time curves is performed. The calculated travel time curves are inverted as many times as necessary to minimize the error between the calculated and observed travel time curves by adjusting the layered velocity model. Then the 2D tomography of the medium is reconstructed from the best fitting travel time curves. The 2D tomography reflects the structure of subsoil and its properties (Forte and Pipan 2008, Polymenakos et al. 2005).

Acquisition and Data Processing

We explored the lot SM-15-1 of the plant-breeding field San Martín of the ChAU. This lot is a 2.18 ha trapezoidal-tilled land with scare vegetation less than a meter high. It is bordered to the N by Av. Molino Rojo, to the W by Av. Benito Juárez South and to the E and S by a flat, 7.5 m wide dirt road slightly higher than the

lot and it has concrete posts close to water intakes. The small-holding is enclosed to the N by a wire mesh and to the W by a metallic fence with a wire mesh. It is noteworthy that approximately 250 m N is an overhead power line and that less a meter away from the W fence there is a medium voltage power line and a pedestrian bridge ramp that runs from the middle to the NW corner of the smallholding (Figure 1 bottom).

Magnetometry survey

The magnetometry survey was conducted with a Gem-System GSM-19T Protonic Precession magnetometer with an integrated GPS system; total geomagnetic field readings were taken every second. A Gem-Systems GSM-19 Overhauser magnetometer situated at 19º29´38.86´´N and 98º52´58.16´´W (white dot on profile M9 on Figure 2) was used as the base station taking readings every 30 seconds. The survey was made following the tills on the surface starting at the SW corner and moving E and then W in a zigzag way. At the extremes of the tilled area we moved 8 m N before turning back. The base station data is adjusted with a nonic polynomial function to make a diurnal correction. A strip of the W end of the terrain was removed to minimize the effects of magnetic noise sources, mentioned on the previous paragraph, and to intensify anomalies in the rest of the area.

The magnetic data was interpolated applying Kriging´s method (Golden Software 2002). To enhance magnetic anomalies and to highlight areas of interest on the anomaly map, the post-processed consisted on applying Reduction to Pole (RTP) and two filters: Fast Fourier Transform (FFT) Band Pass filter from 0.1 to 0.3 ms and a Vertical Sobel filter (Iheme 2011, Langel and Hinze 1999, Vincent and Folorunso 2009).

Figure 2 shows the magnetic profiles (M6 to M9) of the most interesting areas of the anomaly map (Figure 4). The magnetic profiles named SM2 to SM5 coincide with the seismic profiles and the details of the magnetic profiles are explained in Table 1. The magnetic profiles were retrieved from the RTP anomaly map (Figure 4) in order to generate a magnetic susceptibility distribution of the subsoil. Since the study area is flat, the elevation is considered constant at 2246 m.a.s.l. Finally a 2D model of the subsoil is generated for each profile with its corresponding RMS error.

Table 1
Seismic (S) and magnetic (M) profiles´ details

Profile	Orientation	Magnetic length [m]	Seismic source	Seismic stack
SM2	SW – NE	88.5	Dynamite	1
SM3	S – N	93.6	Sledgehammer	3
SM4	SE - NW	89.1	Sledgehammer	3
SM5	SW – NE	93.3	Sledgehammer	3
M6	SW – NE	76.3	-	-
M7	SW – NE	78.4	-	-
¬M8	SW – NE	86.5	-	-
M9	W – E	74.6	-	-

SRT survey

In the seismic refraction survey we used a 48-channel Geometrics StrataVisor NZ11 seismometer and 14-Hz vertical OYO-Geospace geophone. Two types of sources were used, an 8 kg sledgehammer vertically impacting on a groundcoupled steel plate and 15 g dynamite packages buried 30-50 cm deep. The seismic profiles consist of two 46 m long overlapping segments and 24 geophones with an interval of 2 m (Figure 3). The sample rate was 0.125 ms. Seismic profiles were georeferenced using a Magellan ProMark 3 GPS. Five shot point locations are spread along each segment and 3 sledgehammer´s impacts were stacked to enhance the signal-to-noise ratio. Profile details are explained in Table 1 and the profiles´ geometry is shown in Figure 3.

Results and Interpretation

The stratigraphic model of the Texcoco Well by Lozano-García and Ortega Guerrero (1998) (see Figure 1 top for location) was used for the analysis and interpretation of the data. This model shows three principal layers in the first 10 m of the subsoil. From the surface down, the first layer is composed of infilled material, followed by a dark gray silt layer and then by an olive gray silt layer.

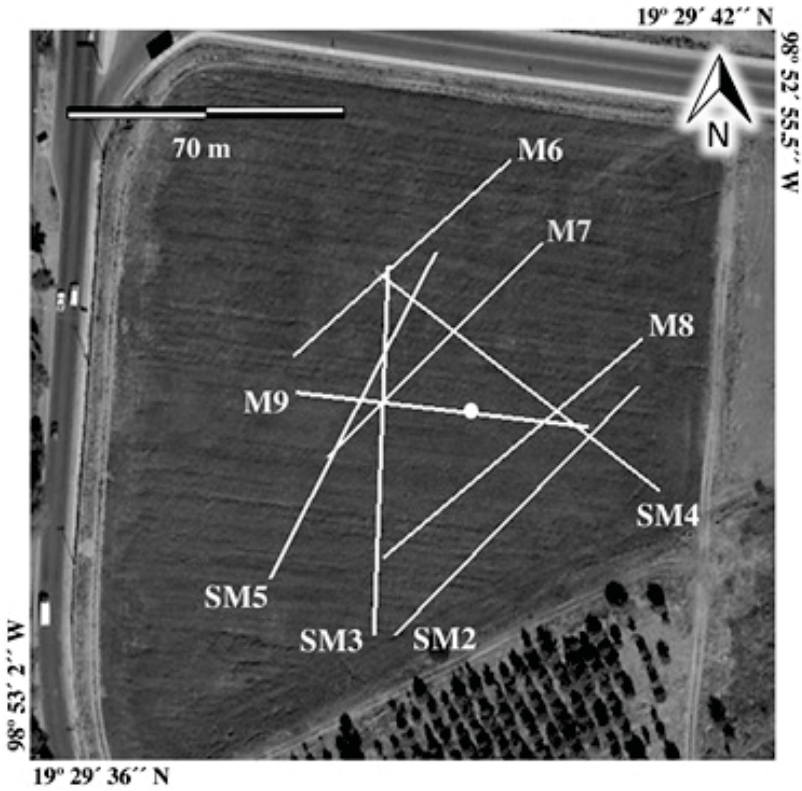

Figure 2. *Seismic (S) and magnetic (M) profiles on the study site. The base station´s location is indivated by the white dot on profile M9.*

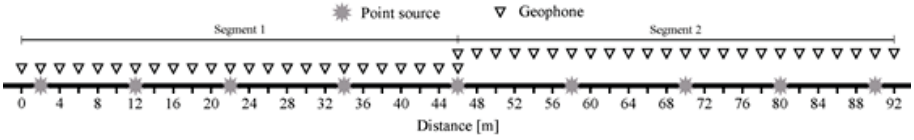

Figure 3. *Seismic profiles´ geometry. Triangles represent the geophones´ location and asterisk the shot points´location. The third shot point of profile 5 is located on 22 m, instead of 24 m as shown in this image.*

During the time of the study the total geomagnetic field in the base station reported variations of 40 *nT* or less. These variations represent a slight perturbation on the Sun-Earth interaction and not a Solar Storm. The RTP anomaly map (Figure 4) shows E – W parallel linear anomalies along with a circular anomaly, 5 to 10 *m* in diameter, on the NW area of the map.

The magnetic models are inverted from a three-layer model, A to C from the bottom up. The magnetic susceptibility, in *SI* units, of layers A is $5.667x10^{-3}$, B is $6.3x10^{-5}$ and C is $1.2x10^{-5}$. Using NOAA´s Magnetic Field Calculators the inclination, declination and the horizontal intensity of the geomagnetic field for the base station´s coordinates are 47.37º, 5.24º and 27735.8 nT respectively. These values are considered to generate the models. The RMS errors of the models are below 0.2 *nT*. An example of a magnetic profile is shown on Figure 5.

On all magnetic profiles interface AB follows the same tendency as the magnetic anomaly curve. This interface on profiles M2, M5, M7 and M8 show an ascend slope with direction SW-NE that can be seen by the interfaces´ ridges and is less prominent towards the E. The ridges, valleys and plateaus of this inter-face vary in dimensions and depth; they are related to high, low and middle values of magnetic field respectively. Interfaces BC are less smooth, most of the time they follows the tendency of interfaces AB but occasionally they seems to have

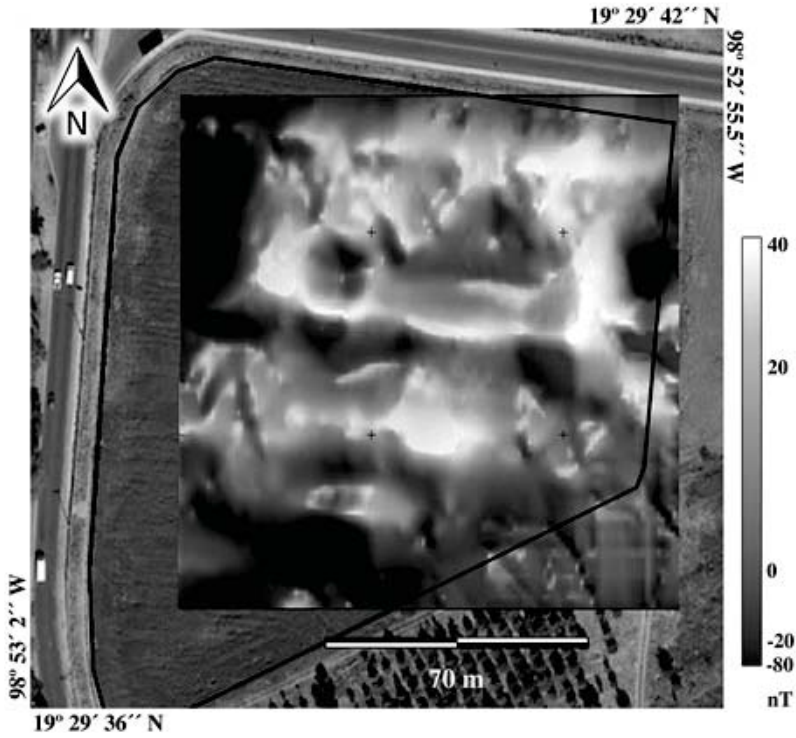

Figure 4. *Reduction to pole anomaly map. The gray scale indicates the magnetic anomaly intensity in nT.*

an offset. The valleys of these interfaces are 3.5 to 8 m long and are on top of the valleys from interfaces AB. Examples of magnetic profiles are shown on Figures 5 and 6 bottom.

Cross-points between magnetic profiles show similarities (see Figures 5 and 6 bottom). Profile M6 shows a deep valley on the same position as the completely circular anomaly, it is related to a valley shown on M7 and could be a Pre-Hispanic or Colonial water well due to its dimensions.

Seismic profile 2 has a 3-layer initial model, the other profiles have a 2-layer initial model. The RMS errors for the Travel Time Inversion are between 0.501 and 1.377 ms, which represent a 1.113% and 2.419% error with respect of the mean value of the reading times, respectively. The 2D Tomographic Inversion RMS errors are between 2.740 and 4.963 ms or between 4.682% and 11.030% with respect of the mean value of the reading times. The seismic velocity range when the sledgehammer is used varies from 165.3 to 698.1 m/s. Dynamite´s seismic

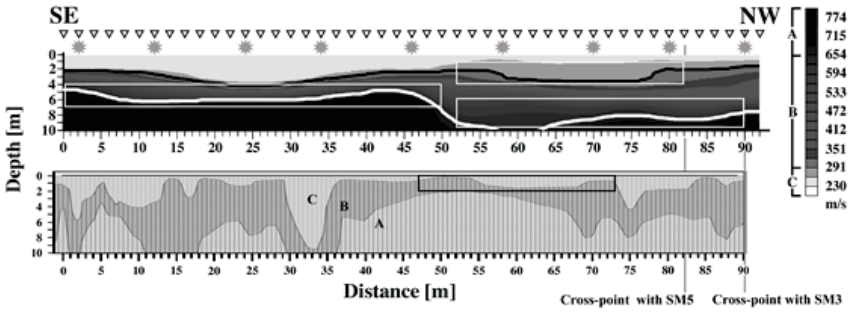

Figure 5. *Correlation between seismic (top) and magnetic (bottom) profiles of profile 4. Magnetic susceptibility values are: A=5.667x10-3, B=6.3x10-5 and C=1.2x10-5. The orientation of the profile is shown on the top, the gray scale indicates the seismic velocity, triangles represent geophones´ locations and asterisk the shot points´ locations. White and black rectangles elcose prominent features.*

velocity range is in average 1.73 times greater than the sledgehammer´s range, between 268 and 1279.75 m/s. Following the same criteria used on the magnetic susceptibility models, the SRT velocity models consist of three layers also. Layer A is the deepest and more consolidated layer, B is the intermediate layer composed by lacustrine sediments slightly consolidated and C is the shal-lowest layer composed by non-consolidate soils. Examples of seismic profiles are shown on Figures 5 and 6 top.

For the objectives of this study, dynamite was not an effective source on soils like Chapingo. Dynamite generates high frequency and high-energy seismic waves that show little or no change at all when passing through

slightly consolidated soils. The information of profile S2 comes from the most consolidated soils located more than 6 m deep, this layer shows similarities with layer A of the models obtained when the sledgehammer was used (S3, S4 and S5).

All seismic profiles show a flat surface between two slight elevations on interfaces BC (see right top rectangle on Figure 5 and left rectangle on Figure 6). If this feature on profiles S2 and S3 are related, this structure has a SW-NE orientation and it is interpreted as an irrigation channel averaging 20.8 m wide and between 2 and 5 m deep bottom. This same orientation is found on magnetic profiles described above.

Profiles S3 and S4 show a depression that is 38 m wide on average and has a depth that varies from approximately 7 m in the E to more than 10 m in the W (see right bottom rectangles on Figure 5). This structure has a SE-NW orientation and is interpreted as a riverbed of an ancient river or stream, getting deeper as it approaches Lake Texcoco.

A trapezoidal structure is found on profile S5 between 1 and 2 m deep and is up to 5 m wide and 2 m high (see right rectangle on Figure 6). Profiles S3 and S5

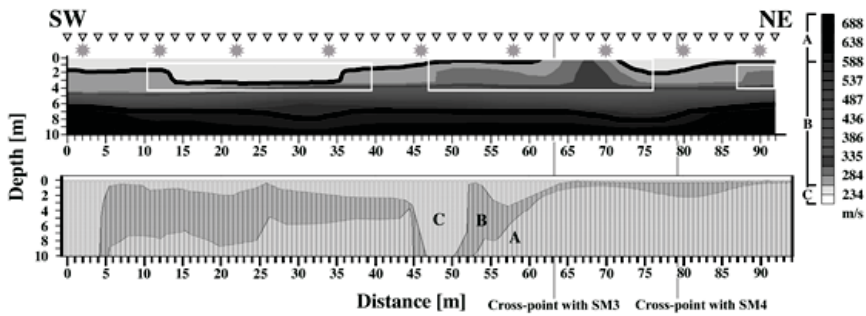

Figure 6. *Correlation between seismic (top) and magnetic (bottom) profiles of profile 5. Magnetic susceptibility values are: A=5.667x10-3, B=6.3x10-5 and C=1.2x10-5. The orientation of the profile is shown on the top, the gray scale indicates the seismic velocity, triangles represent geophones´ locations and asterisk the shot points´ locations. White and black rectangles elcose prominent features.*

show the same 29 m wide and 4 m high irregular structure close to the surface (see middle rectangle on Figure 6). A similar structure is shown on profile S2 sitting on top of a consolidated sediment plateau that is more than 45 m wide; this plateau is next to the depression that has been previously described and is also seen on profile S4. Irregular features are interpreted as mounds or dams and regular features as tlatels and all of them are next to what has been interpreted as channels.

Magnetic and seismic profiles show a few similarities (see right top rectan-gle on seismic profile 4 and the rectangle on magnetic profile 4, Figure 5). The valley on interface BC of S3 is also seen on the same interface of M3. The channel shown in S4 is barely seen on M4 and the cross-point between seismic and magnetic profiles 3 and 4 show the same layer thickness. Features seen on seismic profiles coincide with features in the RTP anomaly map. Interfaces BC of profiles S3, S4 and S5 coincide with the anomaly map. Channels on these same profiles coincide with low values of magnetic field, while regular and irregular structures coincide with high values of magnetic field. These coincidences are not seen on profile S2 due to the source used.

Conclusions

In this work we presented the results of a geophysical survey performed in the lot SM-15-1 of the plant-breeding field San Martín in the Chapingo Autonomous University. The results provide robust elements for an integrated interpretation including the land use and the brief history of the region. We showed that the SRT is an efficient high-resolution technique that details the geometry of buried structures. However, we point out that results of a single geophysical method are not conclusive. Combining the results of these two methods, seismic and magnetic, we showed that the seismic profiles correlate well with the magnetic anomaly map, but they do not correlate with the magnetic profiles. All profiles were modeled with three layers, assuming that seismic velocity and magnetic susceptibility increase with depth. It can be observed in all the profiles, that in the first 10 m of the subsoil the sediments are non-consolidated or they are slightly consolidated, presenting middle to low seis-mic velocities (<745 m/s). Due to the subsoil characteristic in Chapingo and for the objectives of this study, the use of the sledgehammer as a source resulted much more effective than the dynamite.

Ridges, valleys and plateaus of the deepest magnetic interfaces coincide with high, low and middle values of the magnetic anomaly, respectively. For instance, the magnetic anomaly map (Figure 4) shows parallel linear features and a completely circular anomaly interpreted as a water-well. Accordingly, seis-mic profiles´ features (Figures 5 and 6) are interpreted as water or irrigation channels, a SE-NW riverbed, mounds, dams and tlatels. The channels coincide with low magnetic anomaly values (-5 to 15 nT) while regular and irregular structures coincide with high magnetic anomaly values (25 to 40 nT).

The correlation between the two geophysical techniques applied, are a great alternative to map the subsurface and solve archaeological and civil engineer problems in areas where the subsoil has similar characteristics as Chapingo.

Nevertheless, more geophysical studies would be recommended in case of further interest on extending the survey and planning of an excavation.

Acknowledgments

The authors are grateful to the ChAU and in particular to Luis Morett-Alatorre for granting the permissions to work in the study area, to Esteban Hernandez-Quintero, Claudia Arango-Galván and Enrique Cabral-Cano for their advice and support during the field campaign and to Ximena Novo, Luis Salazar Tlaczani, Filiberto Vergara Huerta and José Luis Salas Corrales who were in-volved in the field campaign. This work was partially supported by DGAPA-UNAM project PAPIIT-IN106111. AR acknowledges the Institute of Geop-hysics, Universidad Nacional Autónoma de México for the Scholarship Pro-gram.

References

Aerona, 2012. Refraction Sesmology [PowerPoint slides]. Retrieved February 7, 2013 from http://www.slideserve.com/ aerona/refraction-seismology-chapter-6

Alcocer, J. and Williams W.D., 1996. Historical and recent changes in Lake Texcoco, a saline lake in Mexico. Int. J. Salt Lake Res., 5(1), 45-61.

Arciniega Ceballos, A., Hernandez-Quintero E., Cabral-Cano E., Morett-Alatorre L., Diaz-Molina O., Soler-Arechalde A. and Chavez-Segura R., 2009. Shallow geophysical survey at the archaeological site of San Miguel Tocuila, Basin of Mexico. J. Archaeol. Sci., 36(6), 1199-1205.

Cardarelli, E. and Di Filippo G., 2009. Integrated geophysical methods for the characterization of an archaeological site (Massenzio Basilica – Roman forum, Rome, (Italy). J. Appl. Geophys., 68(4), 508-521.

David A. and Linford N., 2000. Physics and archaeology. Phys.World, 13(5), 27-31.

Fassbinder, J. W.E., 2015. Seeing beneath the farmland, steppe and desert soil: magnetic prospecting and soil magnetism. J. Archaeol. Sci., 56, 85-95.

Forte, E. and Pipan M., 2008. Integrated seismic tomography and ground-penetrating radar (GPS) for high-resolution study of burial mounds (tumu-li). J. Archaeol. Sci., 35(9), 2614-2623.

García, Moll R., 2007. Preclásico Temprano y Medio (2500-400 a.C). Las primeras sociedades agrícolas. Arqueol. Mex., 15(86), 34-39.

Geometrics, 2009. SeisImager/2DTM Manual vr. 3.3. Geometrics Inc, USA, p. 257.

Golden Software, 2002. Surfer User´s Guide: Counting and 3D Surface Mapping for Scientists and Engineers. Golden Software Inc., USA, p. 640.

González, S., Huddart D., Morett-Alatorre L., Arroyo Cabrales J. and Polaco O.J., 2001. Mammoths, volcanism and early humans in the basin of Mexico during the Late

Pleistocene/Early Holocene. In The wold of elephants, proceedings of the 1st Int. Congr., Rome, 704-706.

González, S., Morett-Alatorre L., Huddart D. and Arroyo-Cabrales J., 2006. Mamoths from the Basin of Mexico: Stratigraphy and Radiocarbon Dating. In El hombre temprano en América y sus implicaciones en el poblamiento de la cuenca de México. Primer Simposio Internacional Colección Científica. INAH, Mexico, 263-274.

Flores E. , Hortencia, Cárdenas Soto M. and Lomnitz C., 2009. Respuesta sísmica en el lago de Texcoco. Resultados a partir de registros de movimientos fuertes. Rev. Ing. Sis., (81), 37-51.

Iheme L., 2011. Frecuency Domain Bandpass Filtering for Image Processing [PowerPoint slides]. Retrieved November 13, 2013 from http://es.scribd.com /doc/51981950/ Frequency-Domain-Bandpass-Filtering-for-Image-Processing

Instituto Nacional de Estadística y Geografía: INEGI, 2014a. Anuario estadístico y geográfico por entidad federative 2014, Mexico, p. 774.

Instituto Nacional de Estadística y Geografía: INEGI, 2014b. Cuaderno estadístico y geográfico de la zona metropolitan del Valle de México 2014. México, p. 774.

Jarquín, M.T. and Herrejón Peredo C., 2002. Breve historia del Estado de México. Fondo de Cultura Económica, Mexico City, p. 219.

Jiménez López, J.C., Hernández Flores R., Martínez Sosa G. and Saucedo Arteaga G., 2006. La Mujer del Peñon III. In El hombre temprano en América y sus implicaciones en el poblamiento de la cuenca de México. Primer Simposio Internacional Colección Científica. INAH, Mexico, 49-66.

Langel, R.A. and Hinze W.J., 1998. The magnetic field of the Earth´s Lithosphere: the satellite perspective. Cambridge University Press, USA, p. 450.

López Luján, L., 2007. Clásico (150-600/650 d.C.). La diferenciación campo/ciudad. Arqueol. Mex., 15(86), 44-49.

Lozano García, M. and Ortega-Guerreno B., 1998. Late Quaternary environmental changes of the central part of the Basin of Mexico; correlation between Texcoco and Chalco basins. Rev. Palaeobot. Palynol., 99(2), 77-93.

Matos Moctezuma, E., 2007. Posclásico tardío (1350-1519 d.C.). El dominio mexica. Arqueol. Mex., 15(86), 58-63.

Milsom, J., 2003. Field Geophysics. John Wiley & Sons, England, pp. 232.

Mooser, F., Nairn A.E.M. and Negendank J.F.W., 1974. Palaeomagnetic Investigations of the Tertiary and Quaternary Igneous Rocks: VIII A Palaeomagnetic and Petrologic Study of Volcanics of the Valley of Mexico. Geol. Rundsch., 63(2), 451-483.

Morett-Alatorre, L. and Cabrales J., 2003. El Yacimiento Paleontológico de Tocuila. Imprenta Universitaria, Universidad Autónoma Chapingo, Mexico, p. 33.

Nalda, E., 2007. Epiclásico (650-900 d.C.). Caída de Teotihuacan y nuevas formas de organización. Arqueol. Mex., 15(86), 50-53.

Oberman, A., 2012. Part I: Seismic Refraction [PowerPoint slides]. Retrieved February 7, 2013, from http://isterre.fr/annuaire/pages-web-du-personnel/anneobermann/ Teaching,1310

Padilla y Sánchez, R.J., 1989. Geology and tectonics of the basin of Mexico and their

relationship with the damage caused by the earthquakes of September 1985. Int. J. Min. Geol. Eng., 7(1), 17-28.

Parsons, J.R., 1971. Prehistoric Settlement Patterns in the Texcoco Region, Mexico. Univ. of Michigan Museum, USA, p. 447.

Parsons, J.R. and Morett A. L., 2004. Recursos Acuáticos en la Subsistencia Azteca. Cazadores, Pescadores y Recolectores. Arqueol. Mex., 12(68), 38-43.

Parsons, J.R., 2007. Posclásico Temprano y Medio (900-1350 d.C.). Época de transición. Arqueol. Mex., 15(86), 54-57.

Pérez Campa, M.A., 2007. Preclásico Tardío (400 a.C.-200 d.C.). Las primeras ciudades. Arqueol. Mex., 15(86), 40-43.

Polaco, O.J. and Arroyo-Cabrales J., 2001. El ambiente durante el poblamiento de América. Arqueol. Mex., 9(52), 30-35.

Polymenakos L., Papamarinopoulos S., Miltiadou A. and Charkiolakis N., 2005. Investigation of the foundations of a Byzantine church by three-dimensional seismic tomography. J. Appl. Geophys., 57(2), 81-93.

Pompa y Padilla, J.A., 2006. Los antiguos pobladores de México: evidencia osteológica. In El hombre temprano en América y sus implicaciones en el poblamiento de la cuenca de México. Primer Simposio Internacional Colección Científica. INAH, Mexico, 17-22.

Rojas Rabiela, T., 2004. Las Cuencas Lacustres del Altiplano Central. Arqueol. Mex., 12(68), 20-27.

Rosas A., 2006. Manuel González: la passion de un Presidente. Retrieved February 20, 2013, from http://anech-chapingo.org.mx/hacienda.html

Sharma, P.V., 1978. Geophysical Methods in Geology. Elsevier Scientific Ltd., USA, p. 428.

Siebe C., Schaaf P. and Urrutia-Fucugauchi J., 1999. Mammoth bones embed-ded in a late Pleistocene lahar from Popocatépetl volcano, near Tocuila, central Mexico. Geol. Soc. Am. Bull., 110(10), 1550-1562.

Stein, S. and Wysession M., 2003. An Introduction to Seismology, Earthquakes and Earth Structure. Blackwell Publishing, Singapore, p. 512.

Telford, W.M., Geldart L.P., Sheriff R.E. and Keys D.A., 1978. Applied Geophysics. Cambridge University Press, USA, p. 860.

Vincent O. and Folorunso O., 2009. A Descriptive Algorithm for Sobel Image Edge Detection. In Proceedings of Informing Science & IT Education Conference, (InSite), USA, 97-107.